Electronic Supplementary Information

Extending shelf-life of precursor solutions and inhibiting light-indued oxidation of iodides for achieving highly efficient and durable perovskite solar cells

Weijian Tang [a], Yu Chen [b,*], Ruisen Shi [a], Yihui Wu [c,*], Jingquan Zhang [a,*]

[a] College of Materials Science and Engineering, Sichuan University, Chengdu, 610065, P.R. China

[b] College of Materials and Chemistry & Chemical Engineering, Chengdu University of Technology, Chengdu, 610059, P.R. China.

[c] School of Chemical Engineering, Sichuan University, Chengdu, 610065, P.R. China.

[*]Corresponding author.

E-mail addresses: yuchen7@cdut.edu.cn (Y. Chen), yihuiwu@scu.edu.cn(Y. Wu) zhangjq@scu.edu.cn (J. Zhang)

Experimental

Materials

All the chemicals were used as received. Lead iodide (≥98%) were purchased from Tokyo Chemical Industry; Lead bromide (≥98%,), lithium bis(trifluoromethanesulfonyl)imide salt (Li-TFSI) and 4-tert-butylpyridine (tBP) were purchased from Sigma-Aldrich; Phenethylammonium iodide (PEAI, 99.5%), methylammonium iodine (MAI, 99.9%), formamidinium iodide (FAI, 99.9%), sodium thiosulfate (ST, 99.9%) were purchased from Alfa-Aesar; Lithium bis(trifluoromethanesulfonyl)imide salt (Li-TFSI) and 4-tert-butylpyridine (tBP) were purchased from Sigma-Aldrich. Dimethylformamide (DMF), dimethyl sulfoxide (DMSO), chlorobenzene (CB), isopropyl alcohol (IPA) and acetonitrile were purchased from Sigma-Aldrich and used without purification.

Device Fabrication

Devices were fabricated on cleaned and patterned ITO substrates. The 13 mg/mL of SnO_2 nanocrystalline in ethanol solution was spin-coated on ITO substrate at 3000 rpm for 30s, the annealed at 150 °C for 30 min. followed by spin-coating 10 mM of KCl aqueous solution at 3000 rpm for 30 s and annealing at 100 °C for 10 min. Before perovskite deposition, the ITO/SnO_2 substrate was treated by a UV-Ozone for 15 min.

The perovskite layer was deposited by spin-coating method in a nitrogen filled glovebox. For the control sample, the precursor solution is comprised of mixing 622.4 mg of PbI_2, 208.9 mg of FAI, 10.7 mg of MAI, 10.9 mg of CsCl and 8.6 mg of RbI in 1 mL of a mixed solvent (DMF:DMSO = 4:1, v/v), which was stirred for 24 h before use. The perovskite solution was filtered with 0.22 mm PTFE filter. The solution was spin-coated onto SnO_2 substrates by a consecutive two-step spin-coating process at 1000 and 4000 rpm for 10 and 30 s, respectively. 20 seconds into the second step, 110 μL of anisole was deposited onto the substrate. For the ST-containing sample, a 0.01 mg/ml of ST were added directly into the perovskite precursor ink. Afterward, the substrate was annealed at 110 °C for 30 min. After cooling down to room temperature, a 5 mg/mL of PEAI/IPA solution was spin-coated at 5000 rpm for 30 s and no annealing was required. Hole transport material solution was spin-coated onto perovskite films at 5000 rpm for 30 s in glove box, and the solution of Spiro-OMeTAD/chlorobenzene (72.3 mg mL^{-1}) was prepared by adding 28.8 μL 4-tert-butylpyridine and 17.5 μL Li-TFSI/acetonitrile (520 mg mL^{-1}). Finally, 10 nm of MoO_3 and 100 nm of Au electrode were deposited by thermal evaporation.

Characterizations

The surface and cross-sectional morphology were disclosed by a Titachi S5200 field-emission scanning electron microscopy (Hitachi High Technologies Corporation). The UV-visible absorption spectra of the solution and thin films were measured using an PerkinElmer Lambda 950 UV-vis spectrophotometer. The in-situ UV-vis absorption spectroscopy was recorded with Puguangweishi equipped deuterium light sources from 300 nm to 1100 nm in absorbance mode. The perovskite precursor solution was static spreading on the ITO substrate, and it was spun at 1000 rpm for 10 seconds followed by 5000 rpm for 50 seconds. An antisolvent was dripped for the final five seconds before annealing on an in-situ UV-vis recorder at 110°C for 5 minutes to record its absorption behavior. The XRD patterns of the perovskite films were recorded on Maxima 7000 diffractometer (Shimadzu, Japan) with a Cu Kα radiation (40 kV, 100 mA). The steady PL spectra and time-resolved PL decay of the perovskite films were performed using an FLS980 Series of Fluorescence Spectrometers. For the PL measurement, the excitation source was a monochromatized Xe lamp (peak wavelength at 500 nm with a line width of 1 nm). For TRPL, the excitation source was a supercontinuum pulsed laser sources (YSL SC-PRO) with an excitation wavelength at 600 nm and a repetition rate of 0.1 MHz. The current-voltage characteristics were measured by Keithley 2400 source and the solar simulator with standard AM 1.5G (100 mW/cm^2, Enlitech) under ambient conditions. The *J-V* curves were measured by forward (-0.1 V to 1.5V forward bias) or reverse (1.5 V to -0.1 V) scans. All devices were tested by masking the cells with a metal mask 0.0576 cm^2 in area. Monochromatic external quantum efficiency (EQE) spectra were recorded as functions of wavelength with a monochromatic incident light of 1x10^{16} photons cm^{-2} in alternating current mode with a bias voltage of 0 V (QE-R3011). The TPC and TPV curves for both devices are detected by Fluxim Paios Spectrometer. The light intensity of the solar simulator was calibrated by a standard silicon solar cell provided by PV Measurements. Electrochemical impedance spectroscopy (EIS) was obtained by using a multi-channel potentiostat (VMP3, Biologic) under dark conditions in the frequency range from 1 MHz to 100 mHz with an AC amplitude of 30 mV. Mott-Schottky analysis were conducted by using a multi-channel potentiometer (VMP3, Biologic) at the frequency of 50 KHz in the applied voltage range from 0 V to 1.5 V with an AC amplitude of 25 mV. UPS and XPS spectra were recorded by a Thermo-Fisher ESCALAB Xi+ system. For UPS measurement, He I ultraviolet radiation source of 21.22 eV was used. For XPS measurements，radiation was produced by a monochromatic 75 W Al Kα excitation centered at 1486.7 eV. The dynamic MPP tracking was carried out in a home-made N_2-filled box under 1 sun continuous illumination (white light LED array) with temperature of ~22 °C

(Multi-Channels Solar Cells Stability Test System, Wuhan 91PVKSolar Technology Co. Ltd, China). The MPPT was automatically recalculated every 2 h by tracking the *J-V* curve.The contact angle (CA) were obtained by Powereach JC 2000D6 and all the samples were measured at 25 °C.

Discussion about the current density difference between $J_{SC, EQE}$ and $J_{SC, IV}$

External quantum efficiency (EQE) is defined as the ratio between the number of photogenerated charge carriers and the number of photons incident on the measured device at a given wavelength, under short-circuit conditions. (*REV SCI INSTRUM,* 2015, 86 013112) It is essential to calculate the integrated current density based on the EQE curve and compare it with the short-circuit current density obtained from the *I-V* curve under AM 1.5 G simulated sunlight exposure.

Therefore, we will discuss in detail the mismatch between J_{SC} in *I-V* ($J_{SC, IV}$) and J_{SC} in EQE ($J_{SC, EQE}$). For ST-treated devices, the value of discrepancy is 6.40 % lower than control devices (7.47 %). It could be the difference between the spectral irradiance of the solar simulator and that of the AM 1.5G spectrum, and calibration of errors in the solar simulator. Then, we used the spectral mismatch factor (MMF) to correct the effects of $J_{SC, IV}$:

$$\mathrm{MMF} = \frac{\int E_{\mathrm{ref}}(\lambda) S_{\mathrm{ref}}(\lambda) d\lambda \int E_{\mathrm{simu}}(\lambda) S_{\mathrm{test}}(\lambda) d\lambda}{\int E_{\mathrm{simu}}(\lambda) S_{\mathrm{ref}}(\lambda) d\lambda \int E_{\mathrm{ref}}(\lambda) S_{\mathrm{test}}(\lambda) d\lambda} \qquad \textbf{Equation S1}$$

where $E_{ref}(\lambda)$ is the spectral irradiance of AM 1.5 G spectrum, $S_{ref}(\lambda)$ is the relative spectral response of the reference solar cell, $E_{simu}(\lambda)$ is the spectral irradiance of solar simulator, $S_{test}(\lambda)$ is the relative spectral response. **Fig. S29** shows test report on spectral irradiance of solar simulator (Enlitech, SS-F5-3A). According the test report, the MMF of the control device is 1.008 while is 1.009 for the ST-treated device. The $J_{sc\,(test,\,AM\,1.5G)}$ can calculate from **Equation S2:**

$$J_{\mathrm{SC\,(test,\,AM1.5G)}} = \frac{J_{\mathrm{test,\,simu}}}{\mathrm{MMF}} \qquad \textbf{Equation S2}$$

The $J_{SC, EQE}$ values of the control device is 6.73 %, which is higher than that of the ST-

treated device (5.57 %). The phenomenon may be that the irradiance during EQE test is only about 2 mW/cm^2, which is much smaller than the irradiance of 100 mW/cm^2. This difference in irradiance results in a large difference in the concentration of photogenerated non-equilibrium carriers produced by the solar cell during the test. In addition, perovskite films have a large number of defects at the interface, leading to the formation of new electronic energy levels in the band gap. Under different illumination conditions, these non-equilibrium carriers are localized by these energy levels. Therefore, a large difference in the concentration of photogenerated non-equilibrium carriers will lead to a significant difference in the compensation of electron energy levels in the band gap, and the transport characteristics of solar cells under light will also be very different.

In addition, differences in J_{SC} measured between the *J-V* current and EQE are also reported by other groups. For example, Han *et al.* reported that the J_{SC}, EQE of perovskite solar cells is 7.4% lower than the $J_{SC,\ IV}$ derived from the *I-V* curve. (*Science*, 2014, 345, 295-298.) In addition, Saliba *et al*. have also conducted a comprehensive discussion on this phenomenon, which is caused by many reasons, including calibration methods, the absorption range of the calibration diode, the difference between the solar simulator and AM 1.5 spectrum. (*Nat. Commun.*,2023, **14,** 5445.)

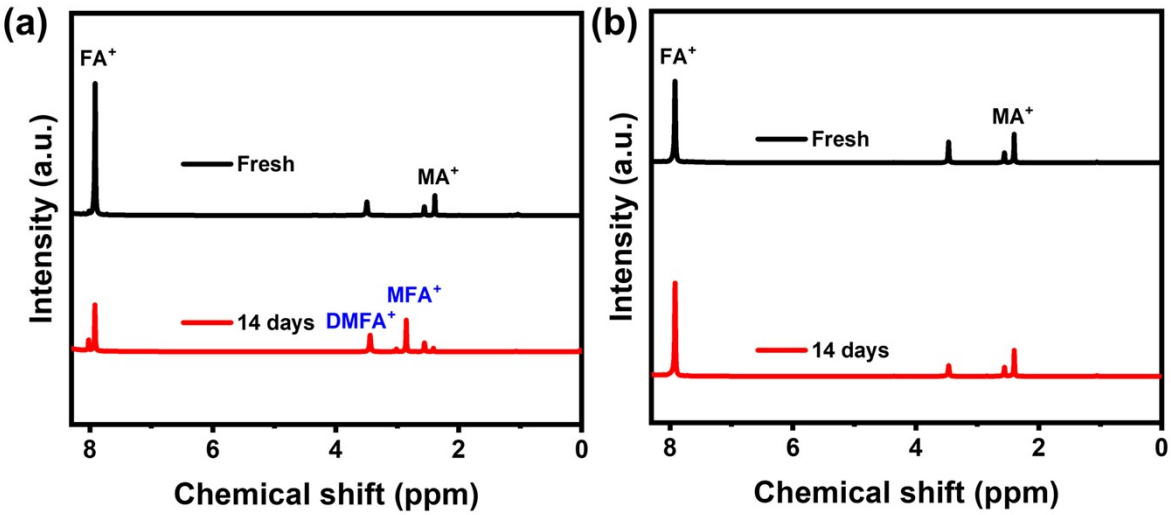

Fig. S1 1H-NMR spectra of the organic cation precursor solution (a) without and (b) with ST under 1 sun continuous light illumination (white light LED array) at different times.

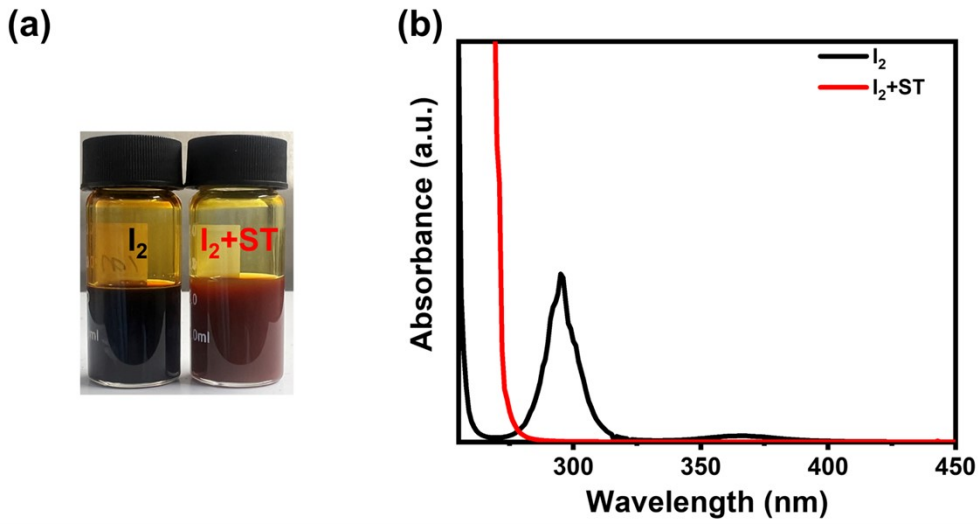

Fig. S2 (a) Photographs of I_2 and I_2-ST solutions; (b) UV-vis absorption spectra of I_2 and I_2-ST solutions (the concentration of I_2 in both solutions was diluted to 10^{-5} M).

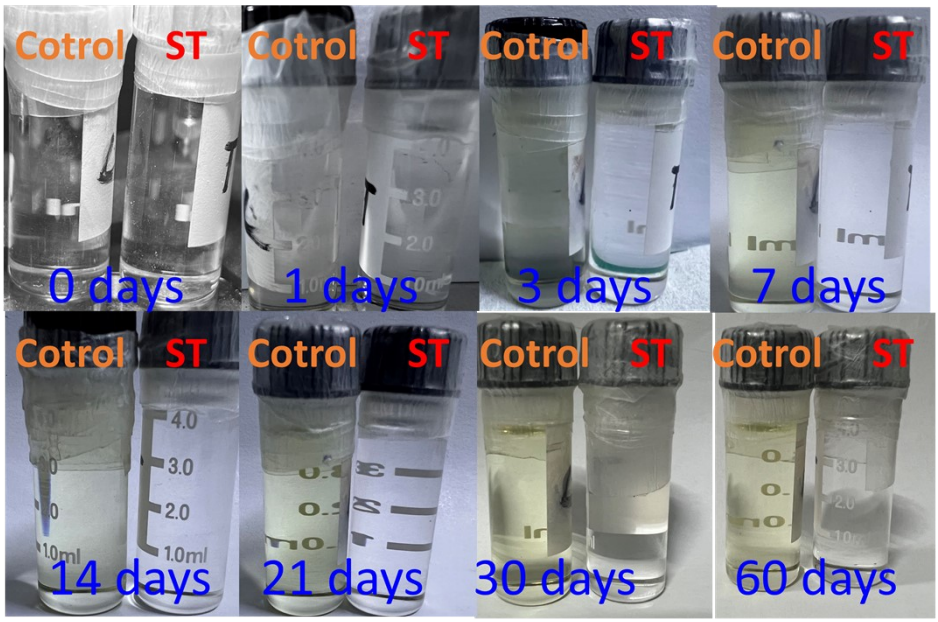

Fig. S3 The image of FAMA solution (DMSO) and FAMA containing ST solution (DMSO) under 1 sun continuous light illumination (white light LED array) at different times.

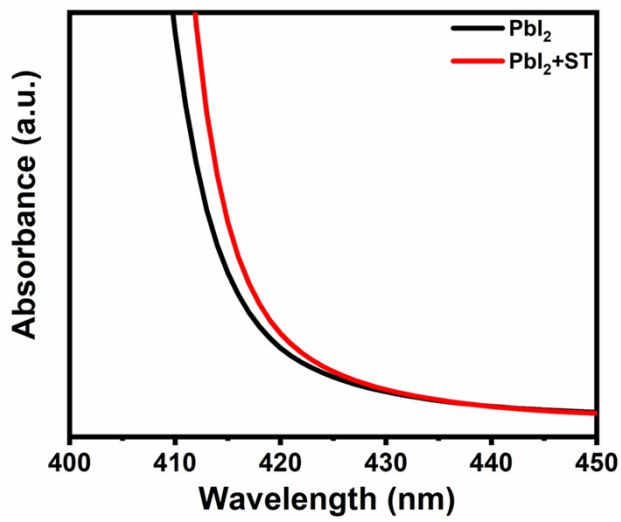

Fig. S4 UV-vis absorption sepectra of PbI_2, PbI_2+ST(solvent: DMSO).

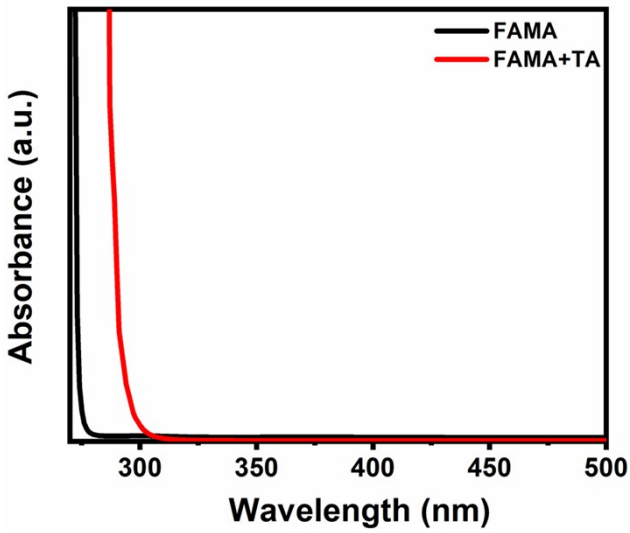

Fig. S5 UV-vis absorption sepectra of FA/MA, FA/MA+ST(solvent: DMSO).

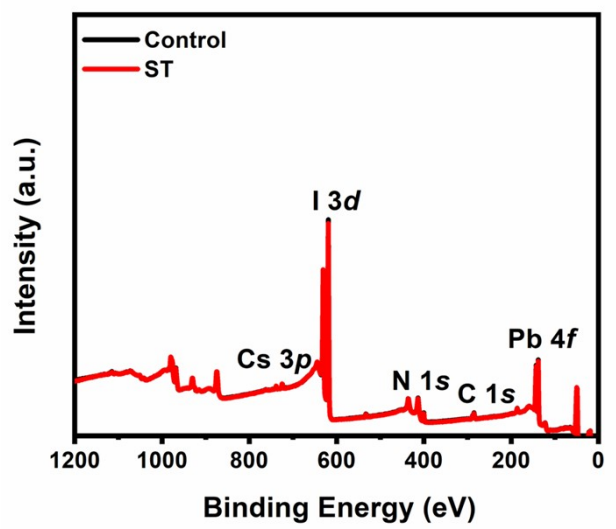

Fig. S6 The XPS spectra of survery, high resolution XPS spectra for perovskite films obtained from the control and the ST-containing precursor solution.

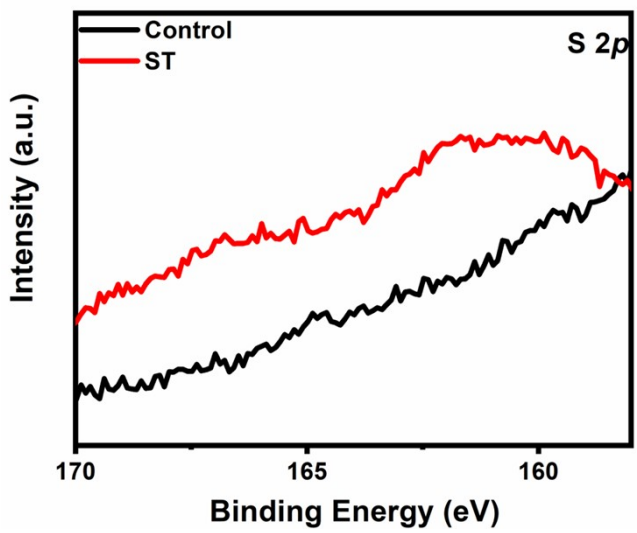

Fig. S7 The XPS spectra of S 2*p* for perovskite films obtained from the control and the ST-containing precursor solution.

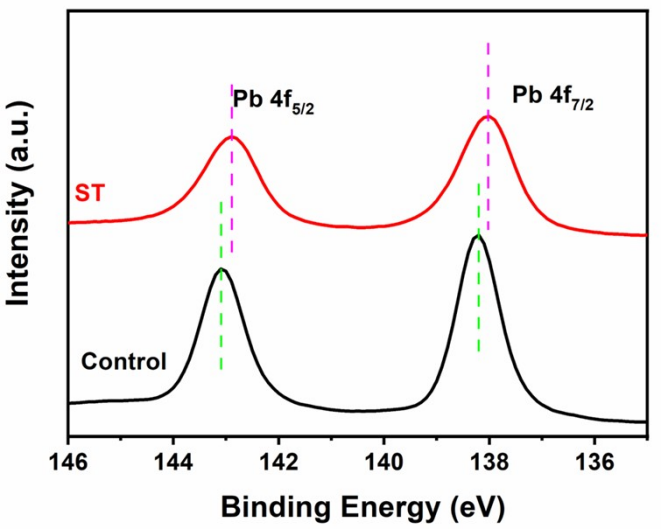

Fig. S8 The XPS spectra of Pb 4*f* for perovskite films obtained from the control and the ST-containing precursor solution.

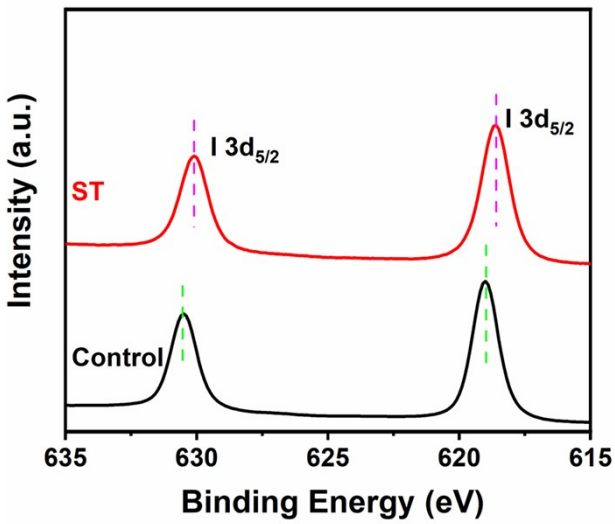

Fig. S9 The XPS spectra of I 3*d* for perovskite films obtained from the control and the ST-containing precursor solution.

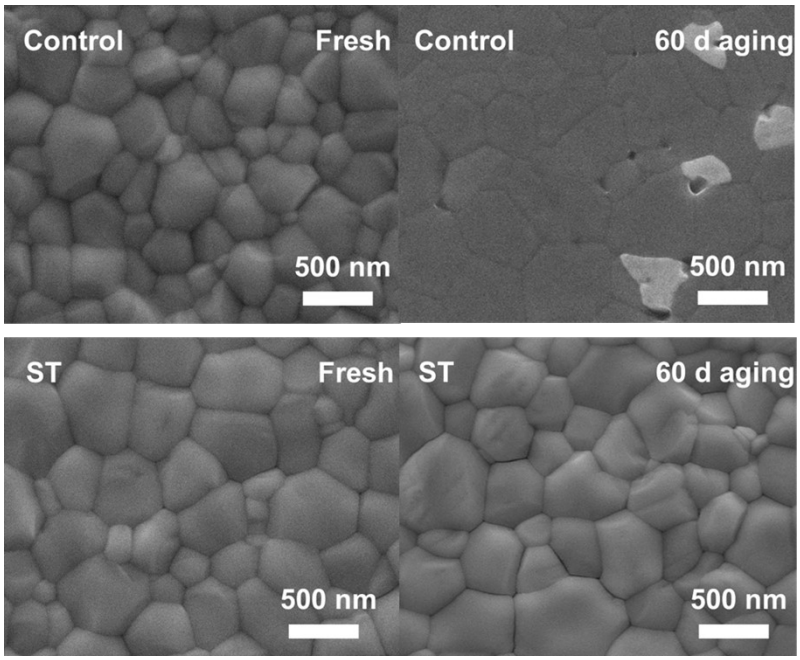

Fig. S10 SEM images of control and ST-treated perovskite films prepared from the fresh and aged perovskite precursor solutions.

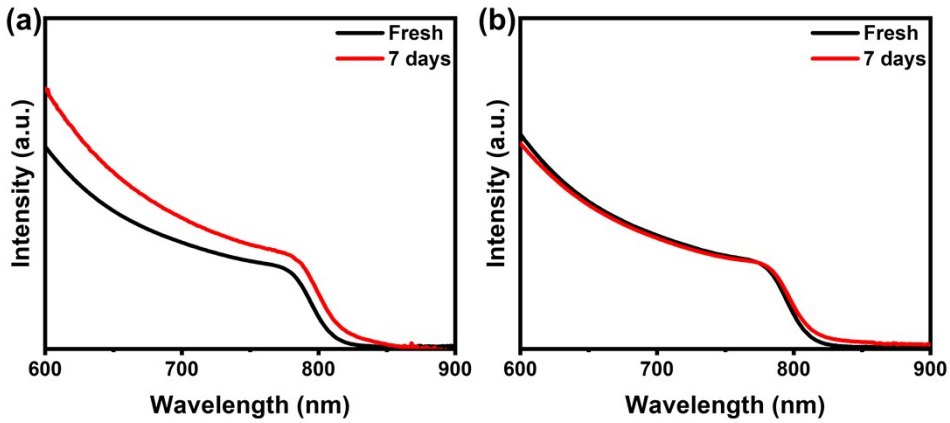

Fig. S11 UV-vis absorption spectra of the perovskite films made by precursor solutions (a) without and (b) with ST under 1 sun continuous light illumination at different times.

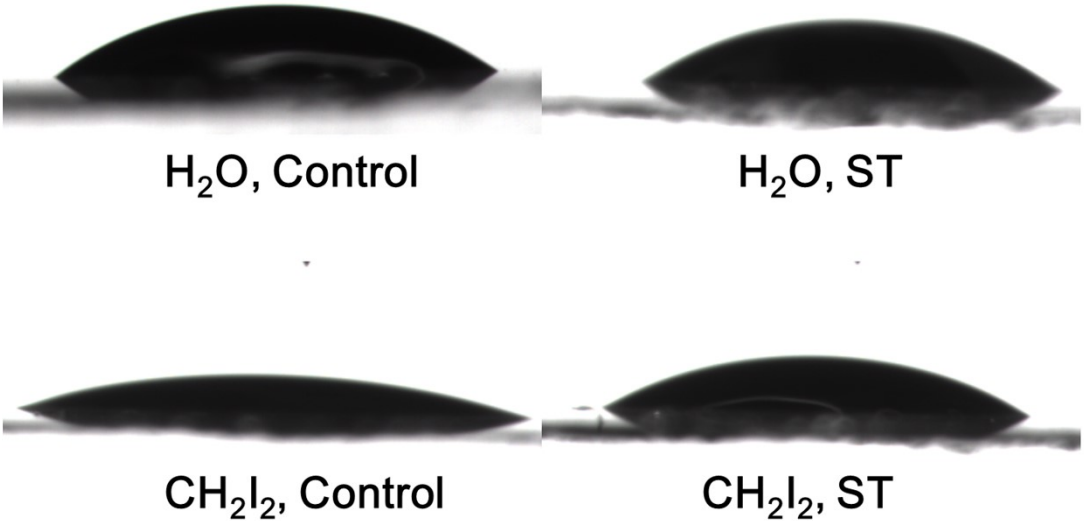

Fig. S12 Contact-angle measurement results for estimating surface free energies. Contact angles of H_2O and diiodomethane (CH_2I_2) on perovskite films without and with ST.

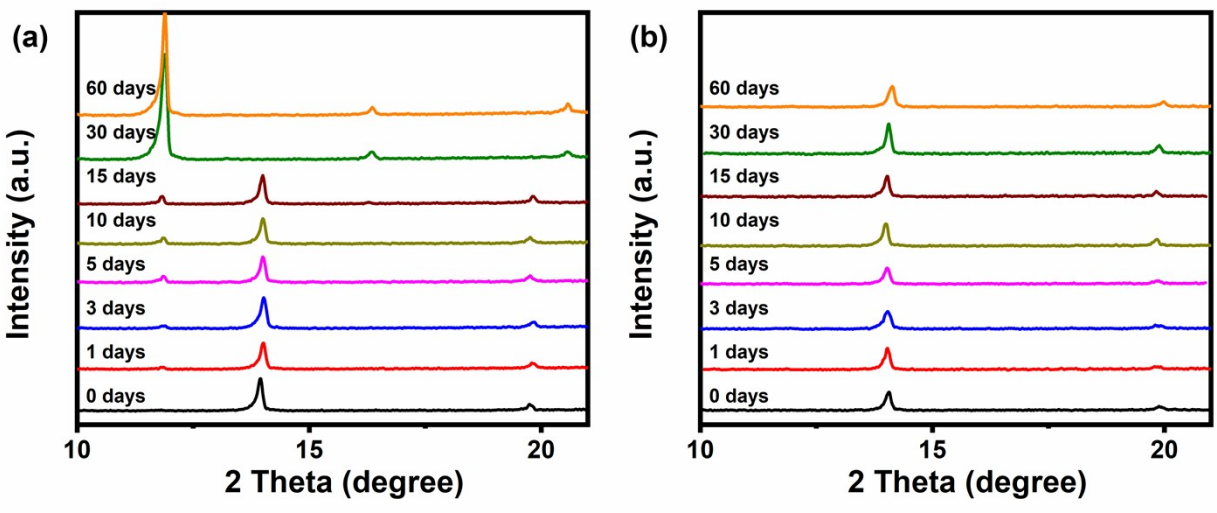

Fig. S13 The XRD spectra of perovskite films obtained from the control (a) and the ST-containing precursor solution (b) under 1 sun continuous light illumination (white light LED array) at different times.

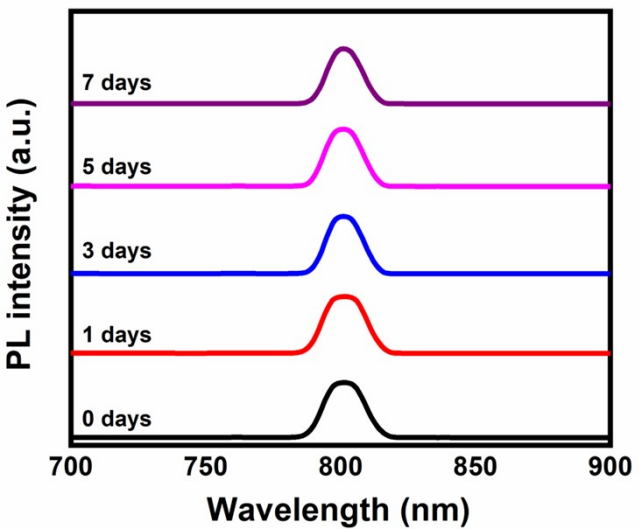

Fig. S14 The PL spectra of perovskite films obtained from the ST-containing precursor solution under 1 sun continuous light illumination (white light LED array) at different times.

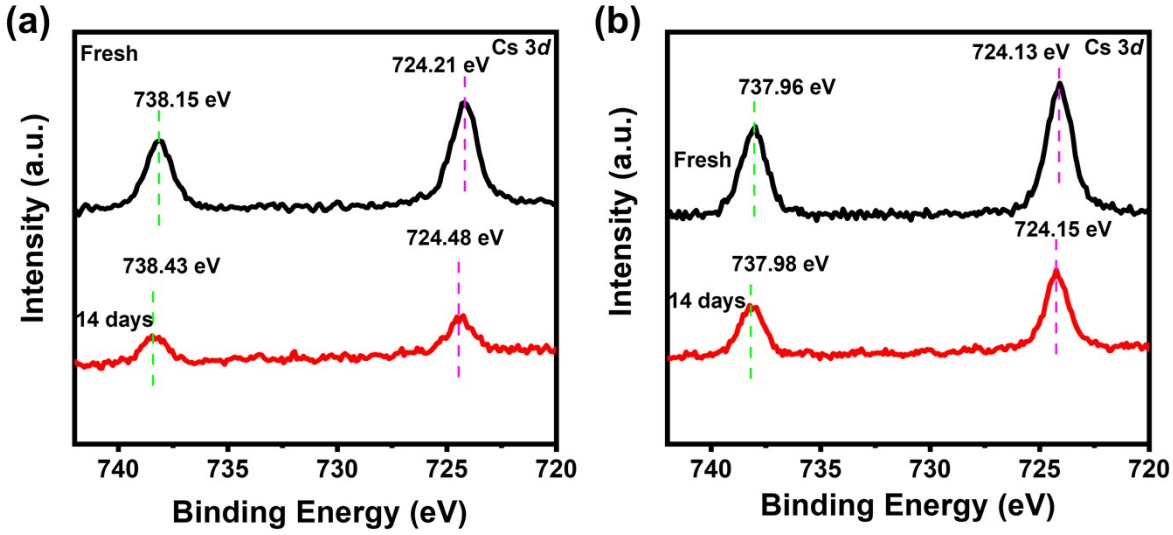

Fig. S15 The XPS spectra of Cs 3*d* for perovskite films obtained from the control (a) and the ST-containing (b) precursor solution.

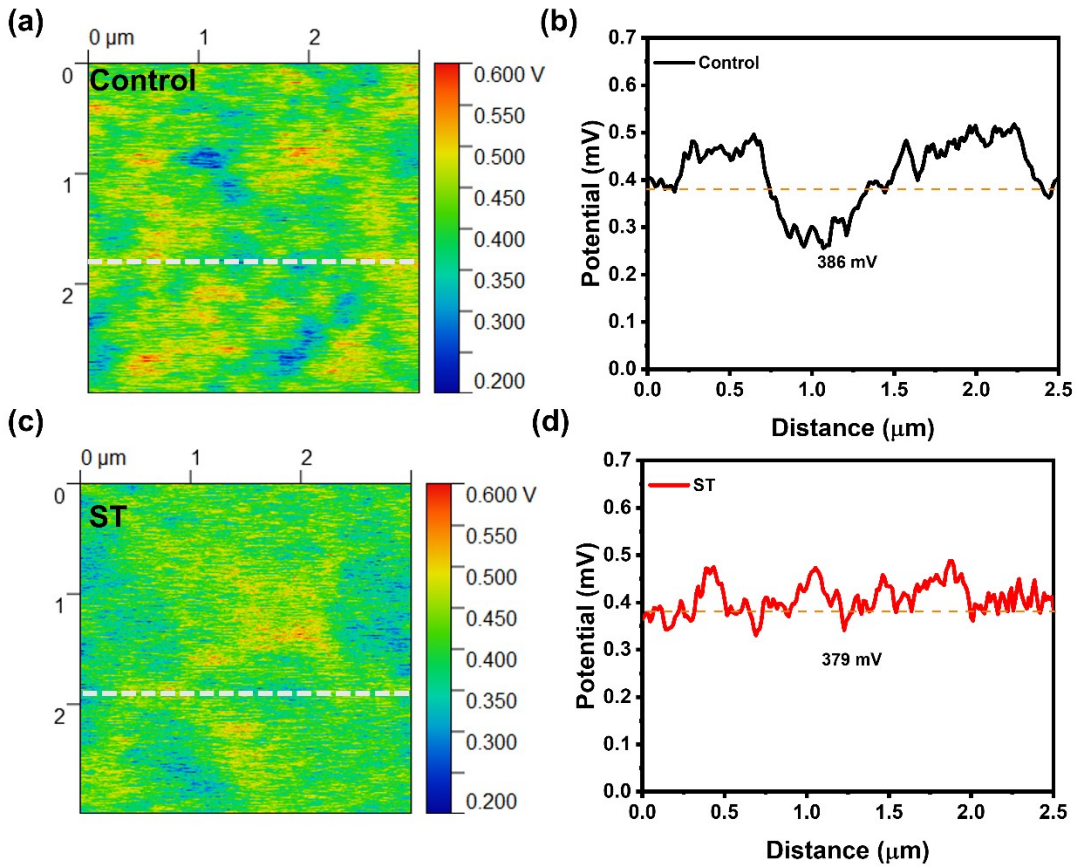

Fig. S16 KPFM images of (a) the control and (c) ST-treated perovskite film. (b, d) CPD changes of the corresponding perovskite films.

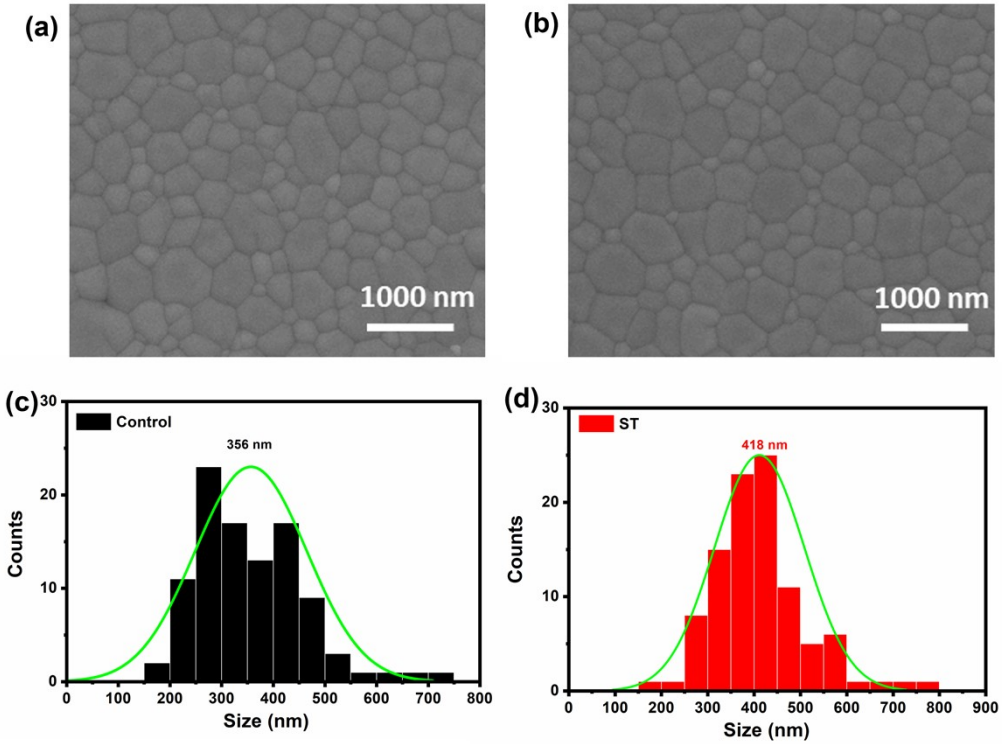

Fig. S17 SEM images and the corresponding grain size distributions of the (a, c) control, (b, d) ST-treated perovskite films.

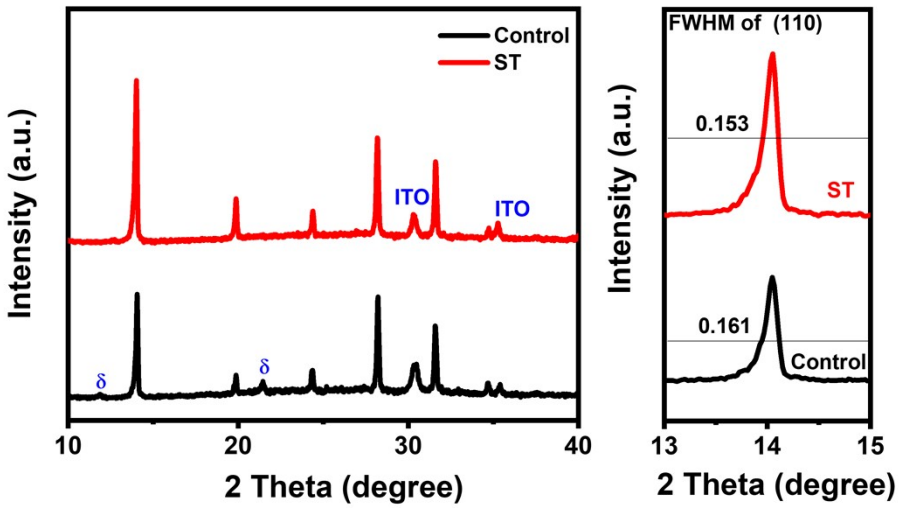

Fig. S18 XRD patterns without and with ST treatment perovskite films.

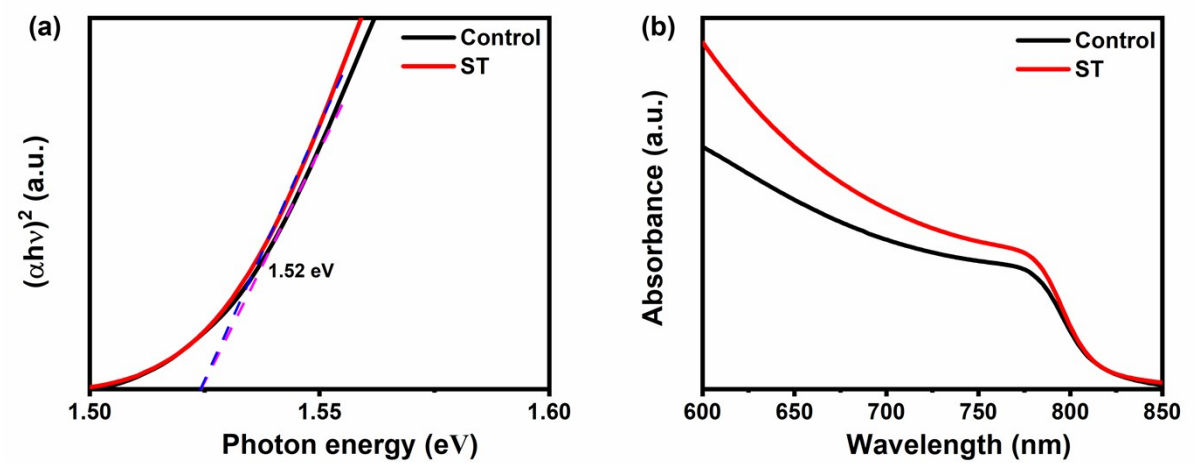

Fig. S19 The UV-vis absorption spectra (a) of perovskite films obtained from the control and the ST-containing precursor solution and the corresponding bandgaps (b) calculated from the UV-vis absorption spectra.

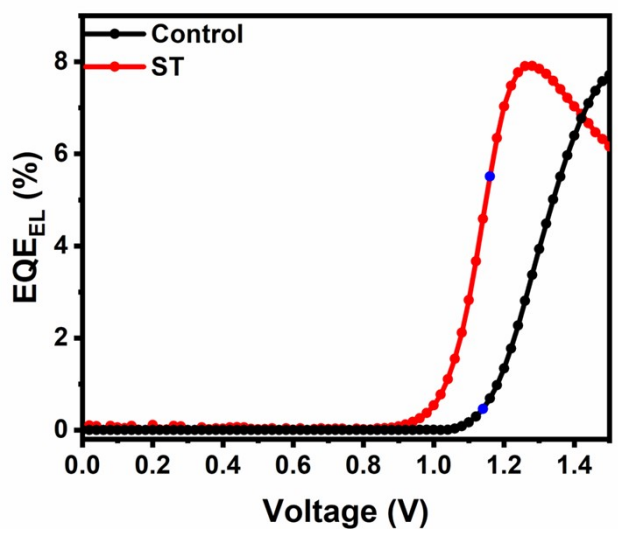

Fig. S20 EQE_{EL} curves of control and ST-treated PSCs.

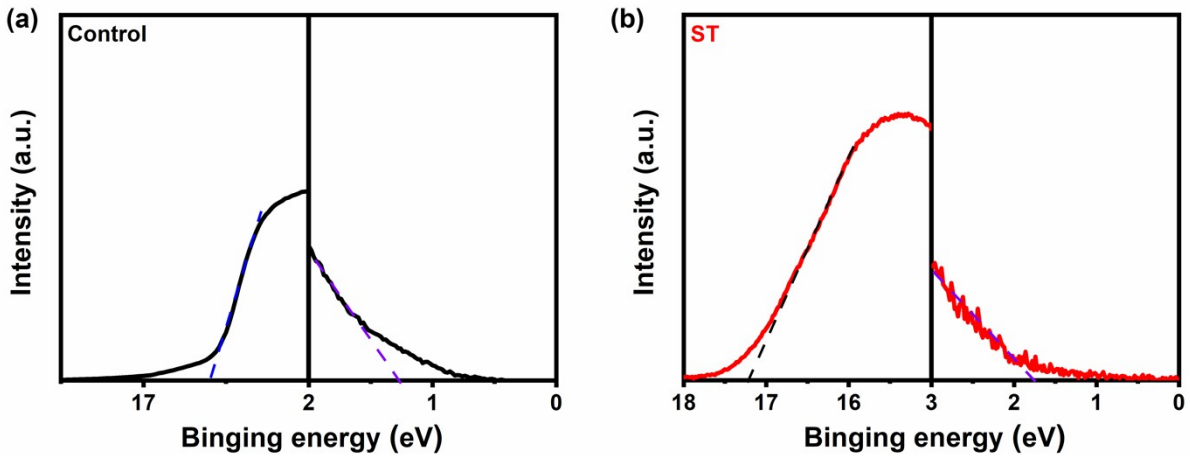

Fig. S21 UPS spectra of the (a) control, (b) ST-treated perovskite films (buried-surface).

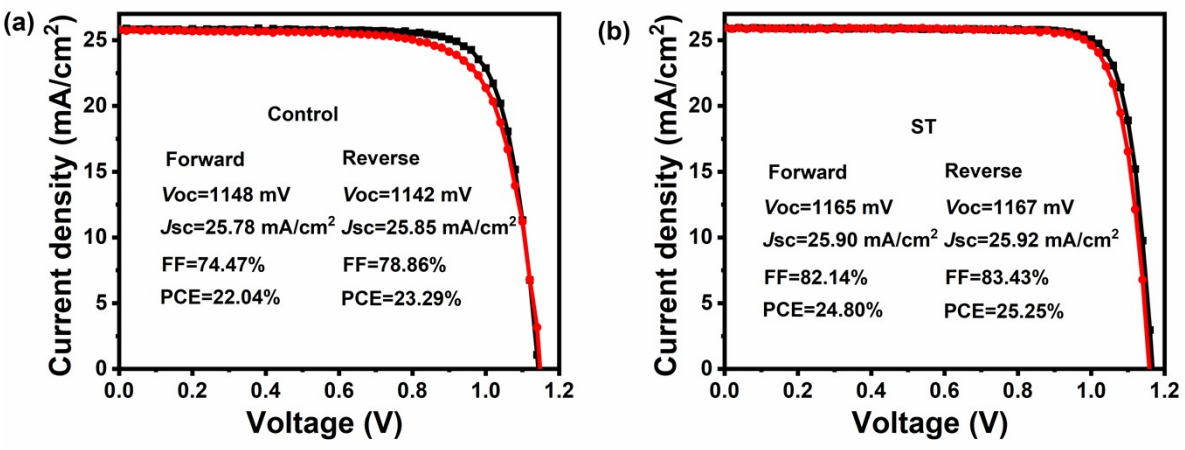

Fig. S22 The *J-V* curves of PSCs with the control and the ST-treatment.

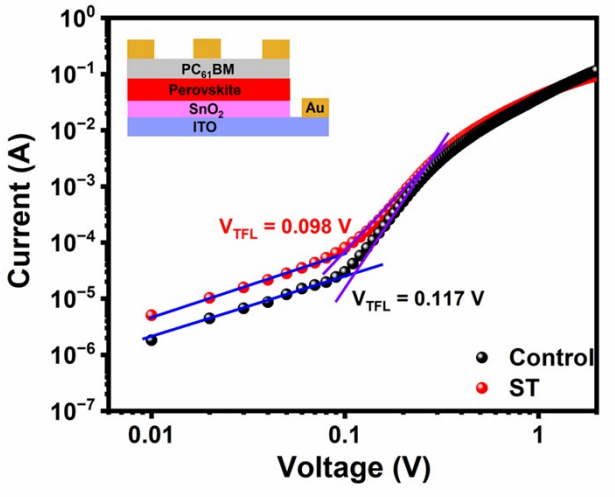

Fig. S23 Dark *I-V* curve for the electron-only structured devices based on the control and ST-treated perovskites.

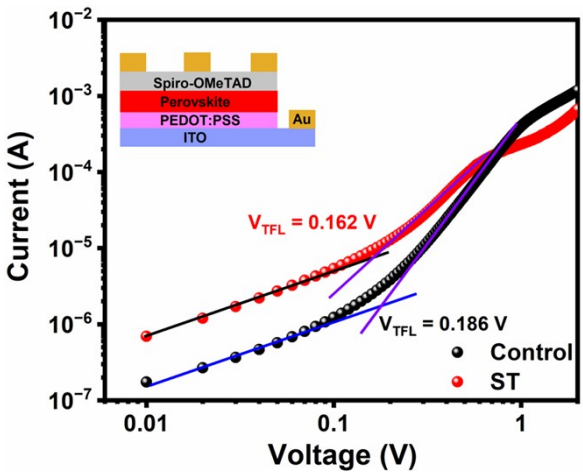

Fig. S24 Dark *I-V* curve for the hole-only structured devices based on the control and ST-treated perovskites.

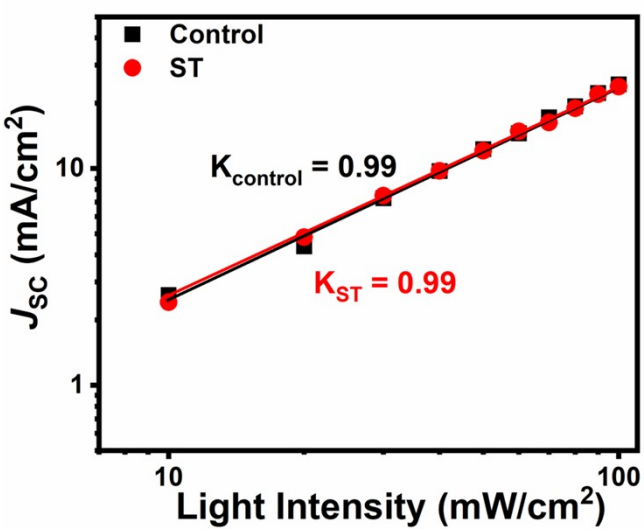

Fig. S25 J_{SC} vs. light intensity based on PSCs with the control and the ST-treatment.

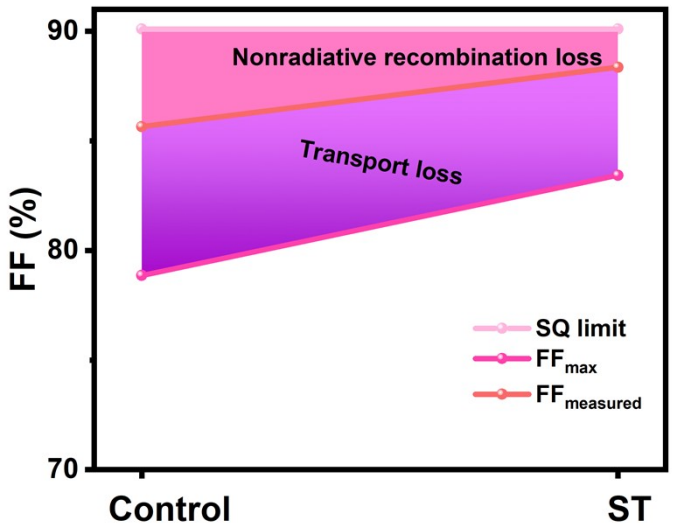

Fig. S26 FF loss curves of control and ST-treated PSCs.

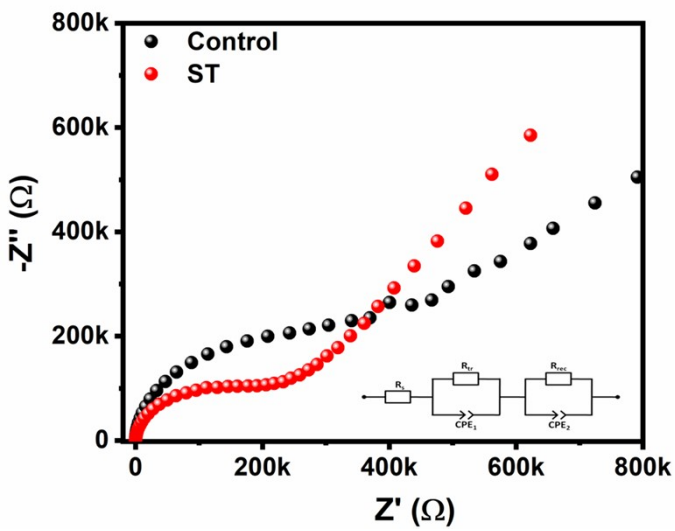

Fig. S27 The EIS plots for the device based on the control and ST-treated perovskites.

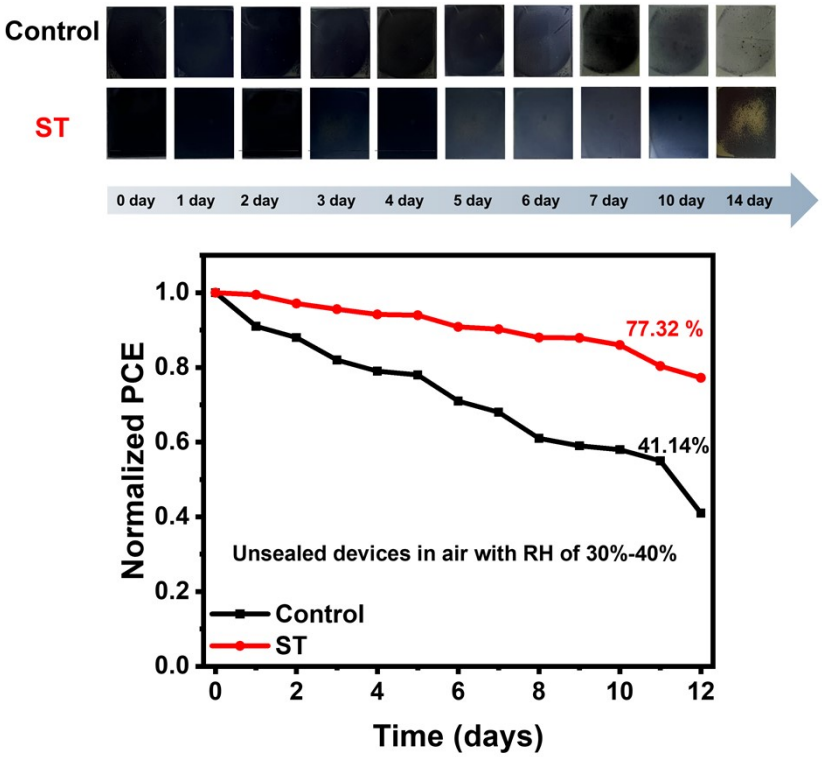

Fig. S28 Humidity stability of perovskite films and PSCs in dark air with RH of 30%-40% at 20 °C.

中国测试技术研究院测试报告　　报告编号　测试字第 202305001179 号

Test Reportof NIMTT　　Report No.

接收日期 Receive Date	2023 年 05 月 08 日	测试日期 Test Date	2023 年 05 月 08 日

本次测试所依据的技术文件
Reference Documents for the Test

JJF1615-2017 太阳模拟器校准规范
IEC 60904-3:2019 Photovoltaic devices - Part 3: Measurement principles for terrestrial photovoltaic (PV) solar devices with reference spectral irradiance data

本次测试所使用的主要仪器设备
Main MeasurementInstruments Used in the Test

名称 Name	编号 No.	测量范围 Measuring Range	不确定度或准确度等级或最大允许误差 Uncertainty or Accuracy Class or Maximum Permissible Error	溯源证书编号 Traceability Certificate No.	有效期至 Due Date
辐照度计	524/10510-0665	(0～1500)W/m^2	U_{rel}=1.8% k=2	GXgf2022-02327	2023-08-28
光纤光谱仪	S1102142U2-S1102143U2	(280～1700)nm	U_{rel}=5.0%～8.5%，k=2	校准 202304003312	2024-04-09
/	/	/	/	/	/

测试地点及环境条件
Location and Environment Conditions

地　点：Location　四川大学（望江校区）第一理科楼，中 226 号

环境温度：Temperature　23℃　湿度：Humidity　50%RH　其它：Others

证书续页（v202101）　第 3 页 共 4 页
Continued Page　Page of

中国测试技术研究院测试报告　　报告编号　测试字第 202305001179 号

Test Reportof NIMTT　　Report No

测 试 结 果

Results of Test

测量状态:被测太阳模拟器辐照度值 1000W/m^2。
被测模拟器(300~1200)nm 相对光谱辐照度，测试结果如下：（光谱辐照度单位：μW·cm^{-2}·nm^{-1}）

波长 (nm)	光谱辐照度	波长 (nm)	光谱辐照度	波长 (nm)	光谱辐照度	波长 (nm)	光谱辐照度)	波长 (nm)	光谱辐照度	波长 (nm)	光谱辐照度
300	0.22	455	21.14	610	27.52	765	35.85	920	23.96	1075	5.43
305	0.27	460	21.58	615	28.96	770	18.27	925	12.13	1080	6.65
310	0.30	465	23.41	620	30.35	775	15.84	930	10.09	1085	8.35
315	0.33	470	25.76	625	30.84	780	14.77	935	11.23	1090	8.34
320	0.41	475	24.55	630	30.90	785	14.58	940	14.85	1095	5.45
325	0.53	480	27.86	635	30.77	790	18.14	945	12.71	1100	2.83
330	0.74	485	30.58	640	30.22	795	15.29	950	15.18	1105	4.05
335	1.38	490	32.87	645	30.45	800	15.85	955	10.99	1110	4.71
340	3.06	495	32.94	650	31.23	805	13.82	960	7.95	1115	4.02
345	5.25	500	29.40	655	29.98	810	14.38	965	8.57	1120	2.85
350	7.72	505	26.47	660	29.78	815	15.22	970	12.70	1125	2.34
355	9.89	510	23.89	665	29.52	820	31.21	975	15.19	1130	2.01
360	10.92	515	22.72	670	29.20	825	93.51	980	41.38	1135	1.81
365	10.89	520	22.44	675	29.20	830	40.72	985	13.49	1140	1.77
370	10.43	525	23.08	680	28.97	835	42.01	990	25.06	1145	1.77
375	9.70	530	24.78	685	30.72	840	20.18	995	27.36	1150	1.88
380	9.44	535	27.23	690	29.64	845	10.11	1000	11.97	1155	1.94
385	9.86	540	29.90	695	26.57	850	7.70	1005	9.98	1160	2.17
390	11.63	545	32.22	700	25.23	855	7.40	1010	12.27	1165	2.75
395	15.15	550	33.15	705	24.15	860	7.74	1015	11.45	1170	3.74
400	19.18	555	32.52	710	25.80	865	8.85	1020	7.60	1175	4.81
405	22.62	560	30.69	715	25.74	870	10.77	1025	5.94	1180	4.36
410	25.02	565	28.58	720	22.74	875	14.31	1030	5.90	1185	3.35
415	25.67	570	26.81	725	21.74	880	42.69	1035	5.44	1190	2.49
420	26.38	575	25.44	730	24.09	885	46.99	1040	5.21	1195	2.05
425	24.97	580	24.62	735	24.35	890	20.42	1045	5.37	1200	1.77
430	24.13	585	24.45	740	23.11	895	41.19	1050	6.32		
435	23.48	590	24.49	745	21.57	900	19.19	1055	6.57		
440	23.18	595	24.71	750	21.36	905	42.49	1060	4.95		
445	22.21	600	25.21	755	20.24	910	14.13	1065	5.10		
450	24.20	605	26.26	760	21.12	915	39.04	1070	5.09		

备注 Note　数据采集积分时间 68.9ms，7 次平均值。

核验员 Checked by　吴伟钢　　测试员 Tested by　康孙李

证书续页（v202101）　第 4 页 共 4 页
Continued Page　Page of

Fig. S29 Test report on spectral irradiance of solar simulator (Enlitech, SS-F5-3A).

Table S1. The contact angles of water (H_2O) and diiodomethane (CH_2I_2) on perovskite films without and with ST treatment.

Probing liquid	control	W ST treatment
H_2O	35°	39°
CH_2I_2	14°	25°

Table S2. Parameters of the TR-PL spectroscopy based on different samples.

Samples	τ_{ave} (ns)	τ_1 (ns)	τ_2 (ns)	A_1	A_2
Glass/perovskite (control)	695.22	1.60	700.37	0.77	0.24
Glass/perovskite (ST)	1621.78	1.50	1625.91	0.78	0.28

Table S3. EIS parameters of the devices based on perovskite films without and with ST treatment.

Devices	R_{tr} (W)	CPE_1 (F)	R_{rec} (W)	CPE_2 (F)
Control	226641	1.68E-8	899946	6.63E-7
ST	339113	1.13E-8	804766	1.49E-7